Supporting Information

Colbert et al. 10.1073/pnas.1303753110

SI Methods

GST Fusion Protein Purification and Binding. GST–Syx1a with and without the L165A/E166A mutation (LE) was expressed from the pGEX vector (GE Healthcare). GST and GST fusion proteins were affinity-purified using glutathione agarose beads and further purified by fast protein liquid chromatography using a MonoQ ion-exchange column (GE Healthcare). For the pull-down experiment, purified Munc18a, GST, or GST–Syx1a ± LE were incubated for 2 h at 4 °C, combined with glutathione agarose beads (final protein concentration ~12 μM), and incubated for an additional 1 h at 4 °C. Samples were spun at 850 × *g* for 5 min at 4 °C, after which supernatant and bead fractions were separated, combined with SDS, and boiled, followed by SDS/PAGE analysis.

Isothermal Titration Calorimetry. Isothermal titration calorimetry was performed as described previously (1).

Fluorescence Anisotropy. Kinetic measurements of the soluble *N*-ethylmaleimide–sensitive factor attachment receptor (SNARE) assembly were performed as described previously (1).

1. Burkhardt P, Hattendorf DA, Weis WI, Fasshauer D (2008) Munc18a controls SNARE assembly through its interaction with the syntaxin N-peptide. *EMBO J* 27(7):923–933.

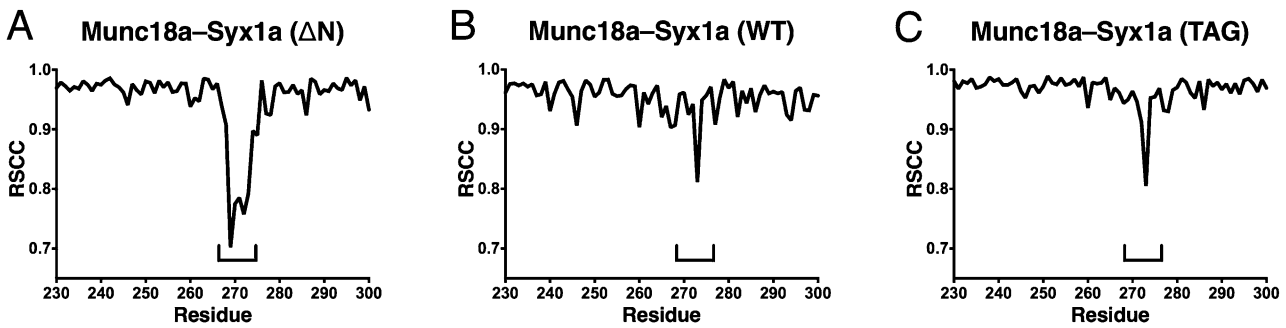

Fig. S1. Comparison of real-space correlation coefficients (RSCCs) for Munc18a domain 3a hairpin loop residues. Plotted are RSCC values for a region of Munc18a domain 3a residues from the Munc18a–Syx1a ΔN (*A*), WT (*B*), and TAG (*C*) structures. β-hairpin loop residues (amino acids 269–274) are designated with a bracket.

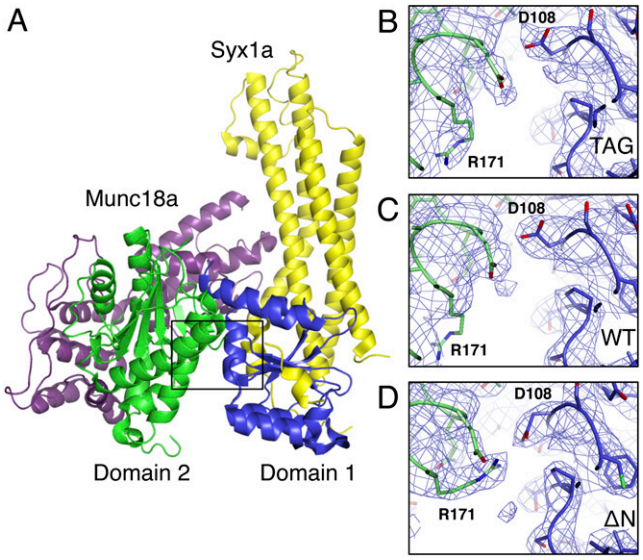

Fig. S2. Interface of Munc18a domains 1 and 2. (*A*) A complex of Munc18a and Syx1a (yellow) oriented to show Munc18a domain 1 (blue) and domain 2 (green). (*B–D*) The boxed region has been enlarged to show the electron density (2Fo-Fc, contoured at 1 σ) for the complex of Munc18a and Syx1a TAG (*B*), Syx1a WT (*C*), and Syx1aΔN (*D*). All 2Fo-Fc maps were generated with a 3.2-Å resolution cutoff. Residues D108 and R171 in Munc18a domains 1 and 2, respectively, form a salt bridge in Munc18a–Syx1aΔN only (detailed in Fig. S3).

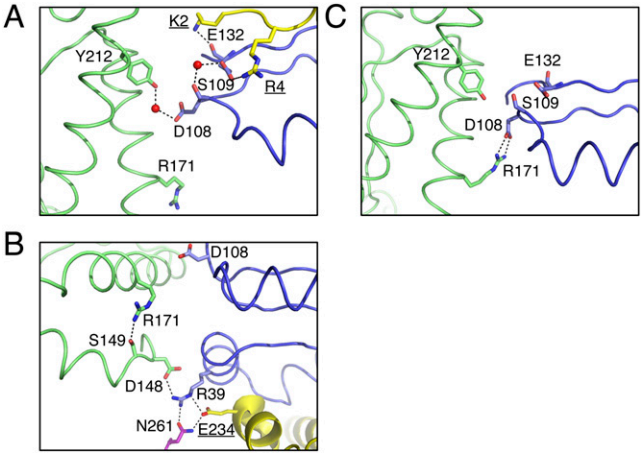

Fig. S3. Possible electrostatic network connecting the Syx1a N-peptide and SNARE-binding regions of Munc18a. (*A*) Syx1a N-peptide (yellow), Munc18a domain 1 (blue) and domain 2 (green) residues, and water molecules (red spheres) are linked through several hydrogen bonds (dashed lines). Syx1a residues are underlined. Starting from the N-peptide site, there are hydrogen bonds between K2 and/or R4 in the Syx1a N-peptide and E132 in Munc18a. Two ordered water molecules coordinate E132, S109, and D108 in Munc18a domain 1. (*B*) The pathway continues through the interface of Munc18a domains 1 and 2, from D108 to N261 (purple) of the SNARE-binding region of Munc18a domain 3a, forming hydrogen bonds with E234 in the Syx1a SNARE domain (yellow). In the Munc18a–Syx1a WT structure, the electron density is weak for R171, possibly indicating that it interacts dynamically with other polar residues when the N-peptide is present. Finally, Munc18a residues R39 and N261 form hydrogen bonds with E234 of the Syx1a SNARE domain. (*C*) Munc18a residues D108 in domain 1 and R171 in domain 2 form a salt bridge in the absence of Syx1a N-peptide. These observations suggest that disruption of the Munc18a–Syx1a N-peptide interaction may lead to a rearrangement of the electrostatic network, with the D108–R171 salt bridge breaking a connection with the Syx1a SNARE domain, thereby enabling SNARE complex formation.

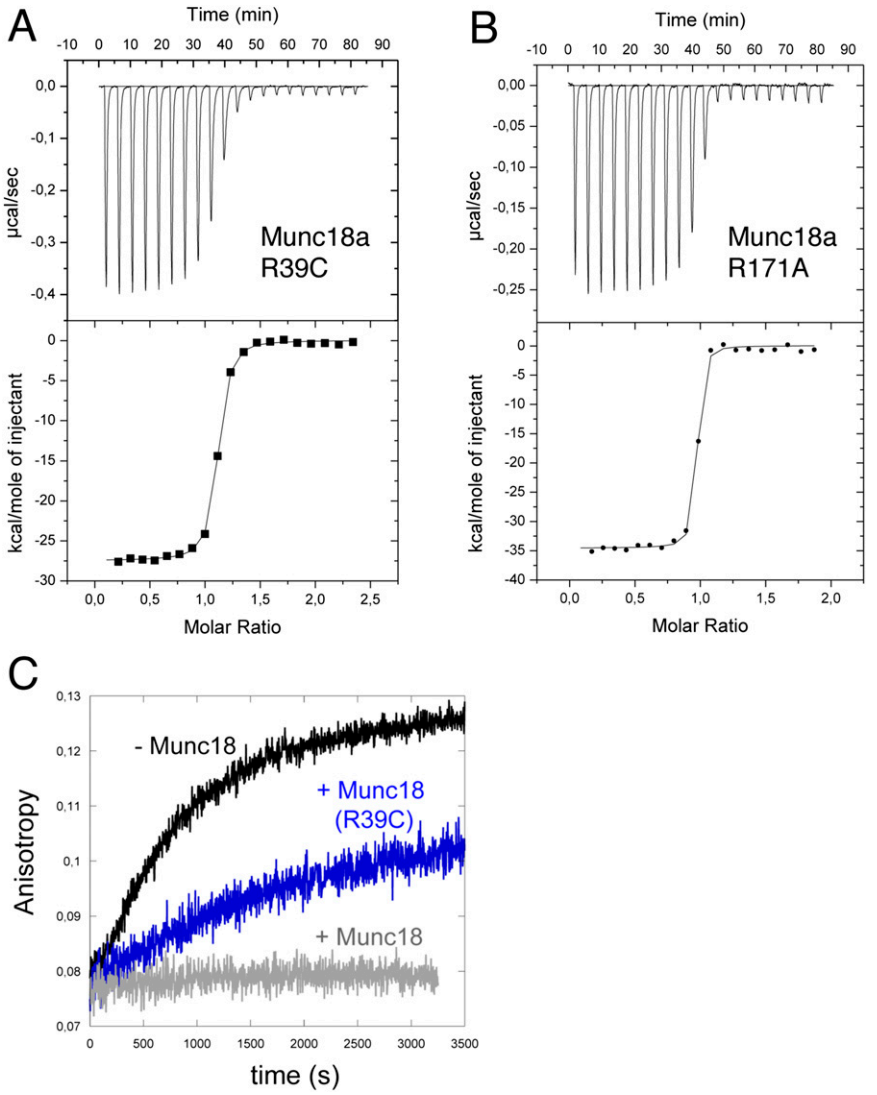

Fig. S4. Effects of Munc18a mutants R39C and R171A on Syx1a binding and SNARE complex formation. (*A*) Syx1a (20–40 μM) was titrated into Munc18a R39C (2.5–4 μM). (*B*) Syx1a (20 μM) was titrated into Munc18a R171A (2.5 μM). (*Upper*) Heat signals corresponding to each injection. (*Lower*) Integrated areas vs. molar ratio of Munc18a–Syx1a. Data were fit to a single binding site model using a nonlinear least squares fit (solid line). Thermodynamic parameters are presented in Table S1. (*C*) SNARE assembly was monitored by an increase in anisotropy of fluorescently labeled VAMP2 (40 nM) when combined with Syx1a (500 nM) and SNAP25 (750 nM) in the absence or presence of Munc18a (750 nM). Munc18a R39C inhibits SNARE complex formation to a lesser degree than Munc18a WT, consistent with its weaker affinity for Syx1a.

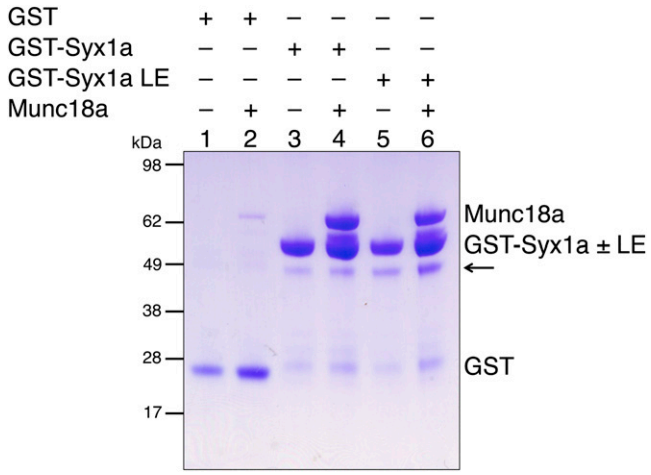

Fig. S5. Interaction of Munc18a with GST–Syx1a ± LE. Bead fractions (combined with SDS and boiled before loading) of GST (lanes 1 and 2), GST–Syx1a WT (lanes 3 and 4), and GST–Syx1a LE (lanes 5 and 6) with and without Munc18a. A small portion of GST–Syx1a ± LE was degraded (arrow), but this had no significant effect on Munc18a binding.

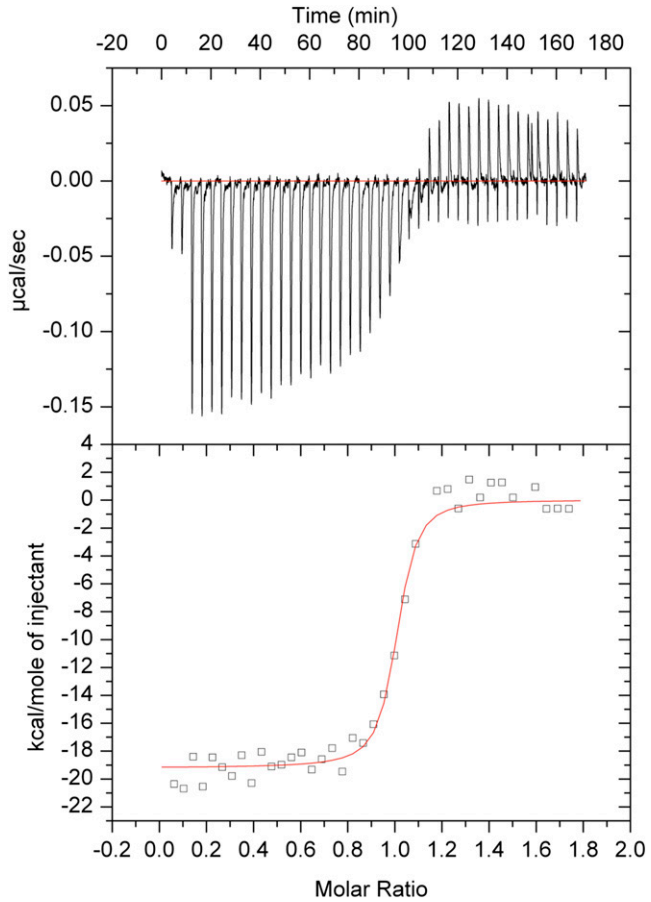

Fig. S6. Calorimetric titrations of Syx1a LE into Munc18a. Syx1a LE (48 μM) was titrated into Munc18a (6 μM). (*Upper*) Heat signals corresponding to each injection. (*Lower*) The integrated areas versus the molar ratio of Munc18a–Syx1a. Data were fit to a single binding site model using a nonlinear least squares fit (solid line). Thermodynamic parameters are presented in Table S3.

Table S1. Thermodynamic parameters of Munc18a R39C and R171A binding Syx1a

Interaction of Syx1a and	K_d, nM	ΔH°, kcal/mol	*n*
Munc18a WT*	1.4 ± 0.3	−34.6 ± 0.2	1.03
Munc18a R171A	0.7 ± 0.2	−36.2 ± 0.2	0.89
Munc18a R39C	6.5 ± 0.6	−27.1 ± 0.1	1.04

*Previously published using the same Syx1a (amino acids 1–262) construct (1).

Table S2. Structural parameters for Munc18a–Syx1a solution structures with and without His_6 tag

	His_6-Munc18a–Syx1a	Munc18a–Syx1a (tag-free)*
D_{max}, Å	111	118
R_g, Å		
Guinier	33.2	35.3
GNOM	33.2	34.9
Theoretical†	33.3	33.3
χ^{2}†	1.8	2.1

D_{max}, maximum interatomic distance; R_g, radius of gyration.
*Edman sequencing indicates that ~22% of total Munc18a in the "tag-free" Munc18a–Syx1a sample includes His_6 tag.
†Derived from CRYSOL (1).

1. Svergun D, Barberato C, Koch MHJ (1995) CRYSOL: A program to evaluate X-ray solution scattering of biological macromolecules from atomic coordinates. *J Appl Cryst* 28:768–773.

Table S3. Munc18a–Syx1a LE thermodynamic parameters

	K_d, nM	ΔH°, kcal/mol	*n*
Munc18a–Syx1a (1–266) LE	10.5 ± 3.0	−19.2 ± 0.2	0.99
Munc18a–Syx1a (1–262) LE	7.7 ± 0.6	−34.8 ± 0.2	0.99

Data in the first row confirm previously published data in the second row (1).

Table S4. R_g value as a function of Munc18a–Syx1a concentration

Concentration, mg/mL	Munc18a–Syx1a (WT)	Munc18a–Syx1a (ΔN)	Munc18a–Syx1a (LE)
1.0	33.6	33.4	34.2
2.0	34.0	33.8	34.1
4.0	34.1	34.8	34.5
6.0	34.4	35.7	34.9

R_g values are expressed in Å.